

A petal resonator volume coil for MR neuroimaging

A.O. Rodríguez*

*Centro de Investigación en Imagenología e Instrumentación Médica, Universidad Autónoma Metropolitana Iztapalapa,
Av. San Rafael Atlixco 186, México, D.F., 09340. México.,
Telephone No./Fax No.: (5255) 8502-4569,
e-mail: arog@xanum.uam.mx*

S.S. Hidalgo**

*Sir Peter Mansfield Magnetic Resonance Centre, School of Physics and Astronomy, The University of Nottingham,
Nottingham NG7 2RD, Britain.*

R. Rojas

*Louisiana State University, Health Science Center, School of Medicine, Department of Radiology,
1542 Tulane Ave., Room 308, New Orleans, LA 70112, USA.*

F.A. Barrios

*Instituto de Neurobiología, UNAM-Juriquilla,
Juriquilla 76230, Querétaro, México.*

Recibido el 8 de junio de 2004; aceptado el 24 de abril de 2006

A variant of the petal resonator (PERES) coil was developed for magnetic resonance neuroimaging applications. It is formed by eight 2 cm-radius petal coils around a central circular-shaped coil with a total radius of 10 cm. As dictated by the theory proposed by Mansfield in 1988, the small coil centers were separated by three times the petal coil radius to avoid mutual inductance between them. The present configuration can easily accommodate a head shape and can be placed nearer the subject to be imaged than other volume coils. Enhancement factor maps were computed to study the coil design performance based on the PERES coil foundations. Coil uniformity was theoretically investigated using the quasi-static approach for various petal coil radii. An 8-petal band coil was built, and in vivo and in vitro experiments were conducted on a clinical MR imager together with standard imaging sequences. Brain images of a healthy volunteer are reported to show the utility of the coil.

Keywords: MR neuroimaging; resonator; coil; sensitivity; uniformity.

Se desarrolló una variante de la antena superficial resonador de pétalo para neuroimagenología por resonancia magnética. El prototipo está constituido por ocho pétalos circulares de 2 cm de radio que se colocan alrededor de una espira circular con un radio de 10 cm. Como lo establece la teoría de la antena PERES, los centros de los pétalos están separados a una distancia de tres veces el radio del pétalo para evitar la inductancia mutua entre ellas. El presente arreglo se ajusta fácilmente a la forma de la cabeza, permitiendo una mejor proximidad comparada con las antenas tradicionales de volumen jaula de perico y el resonador TEM. Se calcularon mapas de mejoramiento para estudiar el desempeño de la antena basada en los fundamentos de la antena PERES. La uniformidad de la antena se estudió de manera teórica usando el enfoque casi estático para el cociente señal a ruido y varios arreglos de pétalos. Se construyó una antena de 8 pétalos y se hicieron experimentos in vivo y in vitro con un sistema de IRM clínico, y secuencias estándares de imagenología. Se reportan imágenes cerebrales para mostrar su viabilidad.

Descriptores: Neuroimagenología RM; resonador; antena; sensibilidad; uniformidad.

PACS: 87.61.-c; 87.61.Ff; 84.32.Hh

1. Introduction

Magnetic resonance imaging (MRI) and in vivo magnetic resonance spectroscopy (MRS) have become essential diagnostic tools in the clinical management of neurological and musculoskeletal disease, and applications in other areas are constantly being defined. This is due to their ability to produce tomographic images at any arbitrary angle with excellent contrast, making them ideal for non-invasively detecting tumors and other neurological diseases. Radio-frequency (RF) coils play a crucial role in the quest for optimal image resolution.

Brain MRI is usually performed with volume coils such as the standard birdcage coil [1], TEM resonator coil [2],

quadrature head coils [3], and planar coils such as phased-array coils [4]. The benefits and pitfalls of all four types of coils for neuroradiological imaging applications have been reviewed [5]. Other types of coils have been introduced very recently based on the micro strip transmission line concept [6] and the SENSE imaging technique [7]. Two main approaches to improve brain image quality at 1.5 Tesla have been traditionally used: a) design of new coils like those mentioned previously, and b) application of intensity-correction algorithms. Naturally, the Signal to Noise Ratio (SNR) can also be greatly increased with magnetic field intensity, but high-field systems (above 1.5 Tesla) are still not widely available in clinics and hospitals around the world. It is particularly important to enhance image quality at 1.5 Tesla, because

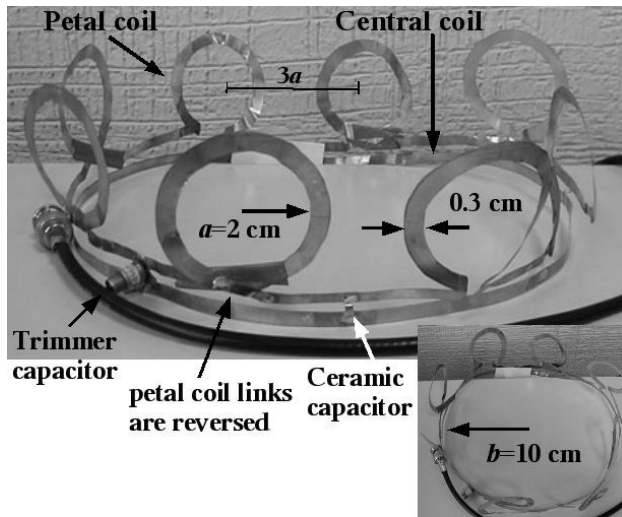


FIGURE 1. Illustration of a petal resonator volume coil prototype with 8 petal coils having a radius of 2 cm and a central coil with a 10-cm radius. The RF phases in each petal must be equal, and its connections have to be alternately reversed so that all the magnetic fields are in phase.

the majority of MR imagers in the world, including Mexican hospitals and clinics [8], use this field intensity.

A novel RF coil design for MR neuroimaging was recently introduced and called the PERES coil [9-10]. This design uses only simple configurations to increase the SNR; it proved to have a higher SNR than the circular-shaped coil, but due to its poor uniformity, an image-correction algorithm is required to improve the image quality. These results motivated the development of a volume coil following the same design principles. An illustration of the coil is shown in Fig. 1. Coil performance was evaluated using enhancement factor maps calculated from Mansfield's SNR model [11]. Coil uniformity was studied theoretically using the quasi-static approach [12]. The prototype coil was tested on a 1.5 Tesla clinical General Electric MR imager. In vitro images were acquired using a General Electric phantom. Transverse images of the brains of healthy volunteers are also presented.

1.1. Theoretical background

Much RF coil development has been done using the trial-and-error approach. However, the principles governing the PERES coil design can actually predict the coil performance and provide us with guidelines to design and build resonator coils for a particular region of interest and at a specific resonant frequency. This can be done through the calculation of enhancement factor maps. The resonator coil SNR can be expressed by [11]:

$$SNR_{PERES} = SNR_b F \tag{1}$$

where

$$F = \left(\frac{Na}{b} \right)^{1/2} \cos(\theta), \tag{2}$$

where a is the petal coil radius, b is the central circular-shaped coil radius, N is the number of connected petal coils, and θ is the polar angle representing the center of the coil of radius a relative to the coil of radius b . F is called the sensitivity enhancement factor. It is assumed that there is no mutual inductance between the coils.

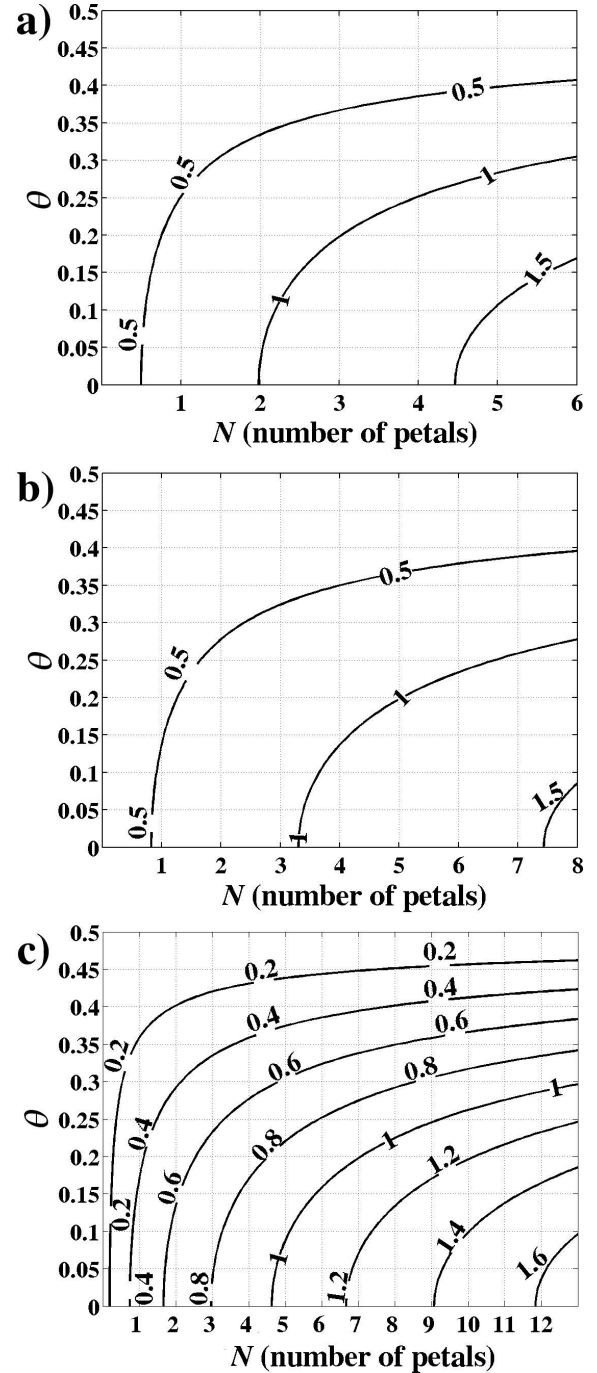


FIGURE 2. Enhancement factor maps for $b/a =$ (a) 3, (b) 5, and (c) 7 were calculated according to Eq. (2), in order to investigate theoretically how que factor F is modified by the size and the number of non-interacting petal coils. Mutual inductance between adjacent petal coils is negligible, since coil centers are $3a$ [a (petal coil radius)] apart.

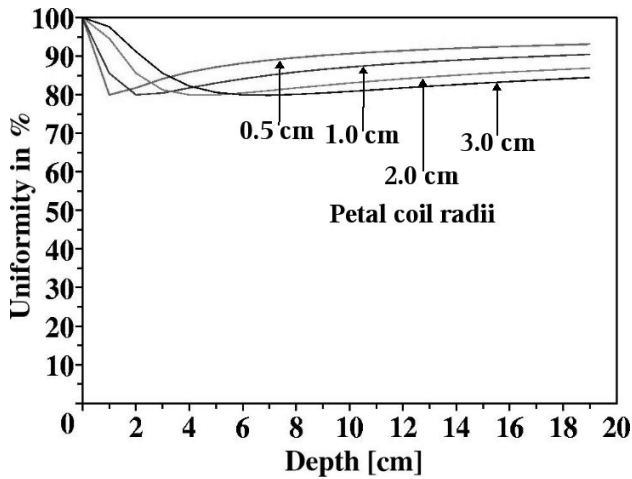


FIGURE 3. Theoretical uniformity profiles of the 8-petal coil prototype considering various petal coil radii. Uniformity greatly improves with increasing the petal radius. There is a trade-off between the penetration capacity and the uniformity, because the mutual inductance is a function of the petal coil radius.

1.1.1. Enhancement factor maps

To guide the development of this coil design, enhancement maps of factor F for different radius ratios in one Cartesian quadrant were calculated from Eq. (2) and are shown in Fig. 2. The actual size of the coil is determined by the ratio a/b . This radius ratio determines the size of the coil design, and there are many possible combinations of a and b . Fractions that are the reciprocals of positive integers (unit fractions) were chosen to simplify this computation process, although other combinations of numbers can be used too. Sometimes representing fractions in this way makes it easier to tell when one is larger than another, so it facilitates the coil construction. To avoid the mutual inductance of adjacent petals, coil centers should be separated by $3a$, as reported [9]. Enhancement maps show the resonator sensitivity as a function of the number of non-interacting petal coils in the form of two-dimensional plots for various radius ratios.

1.1.2. Coil uniformity

To study the coil uniformity, the expression for the percentage integral uniformity, U , reported in [13],

$$U = 100 \frac{SNR_{PERES(max)} - SNR_{PERES(min)}}{SNR_{PERES(max)} + SNR_{PERES(min)}}, \quad (3)$$

and the SNR formula of PERES coil [10] were combined to derive a formula for this coil design:

$$U_{PERES} = \frac{\sqrt{(a^2 + d^2)^3 - 2\sqrt{ad^5}}}{\sqrt{(a^2 + d^2)^3 + 2\sqrt{ad^5}}}, \quad (4)$$

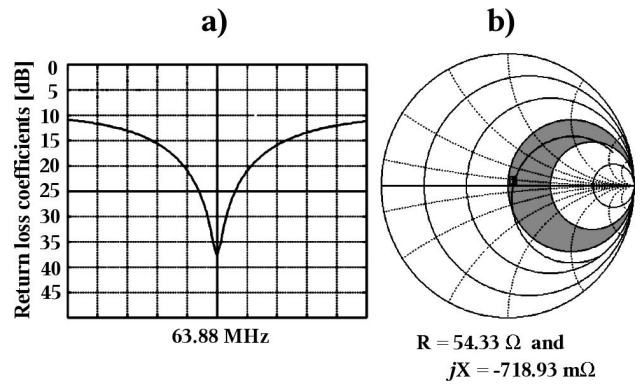


FIGURE 4. Characteristic coil parameters are shown: a) loss return coefficients at 63.88 MHz with an attenuation of 27.36 dB, and b) Smith chart showing a matching impedance, $Z_0 = 53\Omega$ and reactance, $R = 54.33\Omega$ and $jX = -718.93\text{ m}\Omega$ at the resonant frequency.

where d represents the distance from the resonator coil center along a vertical line. Small circle coils can generate high SNR from a particular region of interest, since small regions produce little noise if, for example, petal coils are 5 times smaller than the central circle coil; this coil feature can affect the image quality. Smaller coils can detect higher signals, producing image hyperintensities. This degrades the image quality, making necessary the application of an intensity-correction algorithm. Fig. 3 shows uniformity profiles as a function of petal coil radius and distance d .

2. Method

To develop a coil design with a greater SNR than the circular-shaped coil, the enhancement factor maps in Fig. 2 can be used to select the best parameter to meet this goal. Enhancement maps were plotted for non-interacting petal coils using Eq. (2). In this work, $b = 5a$ was selected, since it provides a SNR higher than unity with a reasonable number of non-interacting petal coils. It can be appreciated that an enhancement factor of 1.265 is obtained for the following coil design parameters: $a = 2$, $b = 10$, and $N = 8$. This resonator design consisted of eight petal coils, each with a 2-cm radius. This array has a band-like geometry in which petal coils are placed symmetrically around a central coil of 10-cm radius. Some of the petal coil links are reversed to add up all the magnetic field contributions coming from the petal coils. Fig. 1 shows an illustration of the coil prototype.

A coaxial transmission line was formed with a 50Ω coaxial cable and the resonator designed to transport the signal to the MR imager. The coaxial-cable central line was attached to the petal coil segment and the grounded screen to the central coil. To tune the coil to the proton resonant frequency of the MR imager, 63.8 MHz, parallel chip capacitors (American Technical Ceramics, NJ) with a 5% tolerance were soldered between the central coil and the elements linking the petal coils. A parallel trimmer capacitor was then soldered for fine tuning and 50Ω matching. The resonant frequencies and quality factor were measured as in Ref. 14. The unloaded

quality factor was 104, whereas for the loaded case (saline solution phantom) it dropped to 80. Fig. 4 shows the loss return of the coil for the resonant frequency and the Smith chart for the coil matching. We tested this resonator volume prototype on a 1.5 T clinical imager (General Electric Medical Systems, Milwaukee, WI). This scanner is equipped with the 5.8 software version. All imaging experiments were run with the surface coil option provided by the manufacturer.

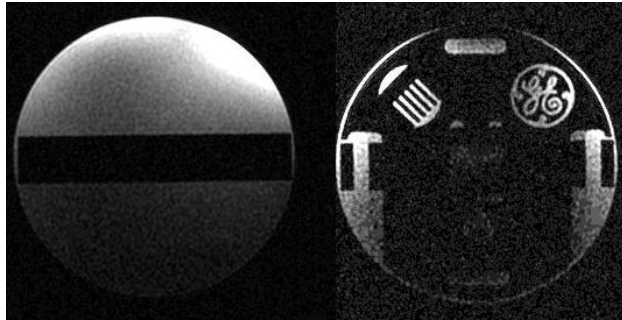


FIGURE 5. T2 images with axial orientation obtained from a General Electric phantom are shown. Both images show poor mutual inductance generated by the petal coils. Relatively poor uniformity is also apparent.

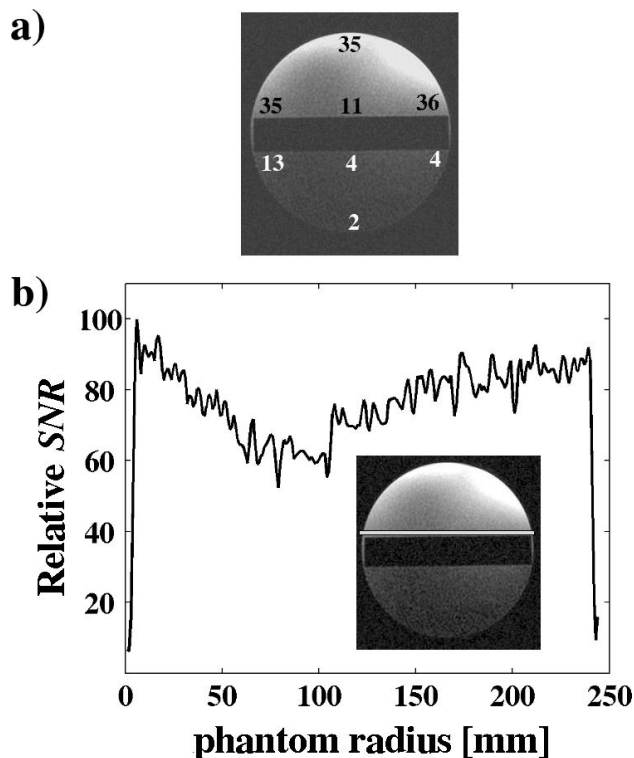


FIGURE 6. a) SNR maps from the coil design and b) SNR profile along the phantom diameter.

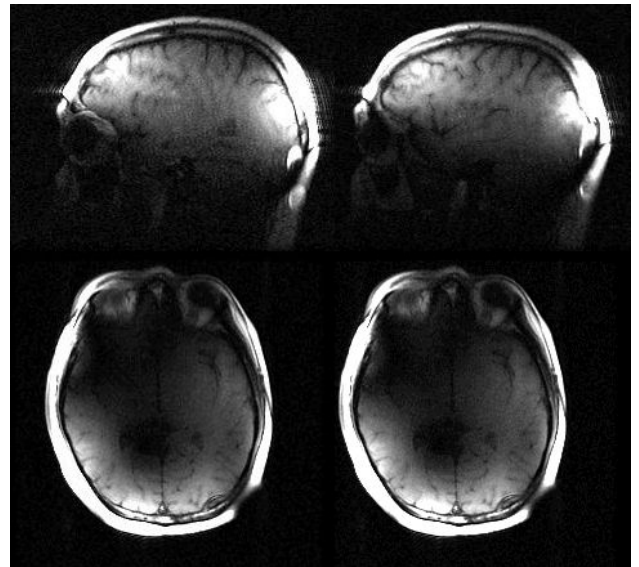


FIGURE 7. Representative T2 -weighted images of a healthy brain. These images were acquired with a clinical fast spin-echo (FSE) sequence. Sagittal brain images are in the upper row, and coronal images are shown in the lower row. Hyperintensities can be observed in both orientations.

3. Results

Prior to obtaining brain images, phantom images were acquired with a General Electric spherical phantom and the petal resonator volume coil. All imaging experiments were run with the surface coil option and standard spin-echo sequences (Fast Spin-Echo). Imaging experiments were conducted, and T2 images were obtained prior to the in vivo imaging experiments. The following imaging acquisition parameters were used for all imaging experiments: TR = 400 ms, TE = 100 ms, FOV = 22 cm, image size = 512 × 512, NEX = 5, in-plane resolution 1 mm, and slice thickness 10 mm. Fig. 5 shows phantom images in different orientations. A SNR map and an axial profile were computed from the phantom images of Fig. 5 and are shown in Fig. 6. Images of a healthy brain were then obtained with the same acquisition parameters previously used for the phantom images. Brain images are shown in Fig. 7.

4. Discussion

The current coil prototype shows that this approach can be an alternative to the trial-and-error method extensively used to develop MRI coils. The number of petal coils becomes an important design feature mainly due to the unwanted mutual inductance. However, the possible configurations of this resonator approach are limitless since not only the number of petal coils but also their shape can be modified. The relevant theoretical information on coil performance can be obtained from the enhancement maps, regarding the optimal number of petal coils that can be accommodated in a specific-size central coil.

The sensitivity plot of Fig. 2b reveals that 3 petal coils is the smallest number required to produce a factor F greater than one, provided that $b = 5a$. Then the SNR grows with the number of petals, but separation between each two centers tends to decrease, and this can cause the undesired effect of mutual inductance. Resonator coil size is a function of the ratio, so extra care should be taken when selecting a particular ratio; larger ratios demand a larger number of petal coils to assure a $SNR > 1.0$. This implies that if the separation between coil centers is not at least $2a$, the undesired interaction of coils will occur and consequently affect the factor Q as defined in Ref. 14. Therefore, maps of the sensitivity factor F in Fig. 2 offer guidelines for optimal design parameters to develop resonator coils with high SNR configurations.

Separation of petal coils was investigated by acquiring phantom images (Fig. 5). The coil-center separation shows that the mutual inductance is practically negligible. Phantom images show that the mutual inductance between the adjacent petals did not degrade the image quality, since the petal coil radii were separated by 3 times the petal-coil radius (a).

Coil tuning and matching is an important issue when building an MRI coil. These parameters determine the resonant frequency and the maximum energy transfer from the coil to the MR imager. Since petal coils are symmetrically located around the central coil, this resonator design is particularly suitable for a good capacitance distribution, because each petal coil can be regarded as a small resonant circuit. To take advantage of this, a chip capacitor was soldered between two petal coils around the whole coil design, offering a well-balanced resonator coil. However, a large number of chip capacitors are a major source of noise, thus altering coil performance and resulting in poor quality images.

The attenuation coefficients of Fig. 4a show that this coil design can achieve good penetration range. This implies that signals from regions reasonably far away from the coil in a straight line can be captured. Despite the complex layout, it could achieve a good matching impedance figure, as shown in Fig. 4b. Impedance and reactance are in good agreement with experimental results previously reported. Impedance and reactance are very sensitive to small deformations of the coil, cold soldering, and low quality electronic components. The resonator coil was mounted on thick cardboard, so handling caused small deformations increasing the coil reactance. Maximum energy transmission cannot, be assured, and consequently, a low image SNR can be detected. To avoid an increment of the reactance and impedance, the coil should be mounted on a non-conducting, rigid surface.

The theoretically acquired profiles of Fig. 3 show that the coil uniformity depends on petal coil size and that uniformity improves as a function of the petal coil radius. There is up to a 20% drop of uniformity for regions near the coil plane, but for distant points a 10% recovery can be observed. As the petal coil radius increases, the uniformity remains almost constant. However, it can also be appreciated that for large petal coil radii, uniformity is regained for regions in the vicinity and parallel to the coil plane.

The petal resonator principles can actually increase the possible combinations to build a coil specifically for a particular region of interest, as in the case of MR neuroimaging. The petal resonator volume coil can achieve the central-shaped coil uniformity by simply increasing the petal coil radius. This petal radius will not increase the mutual inductance present if the coil separation is adequate. Experimental SNR values and the experimental axilla profile of Fig. 6 show that this coil can generate fairly good uniformity.

The current coil design can better fit the shape of the head because of its cap-like configuration. This design can then be placed in close proximity to the region of interest, and high signals can then be obtained. The coil configuration cannot cover the whole of the head; about 80% of a young, healthy volunteer's head could be scanned. This means that it cannot generate images across the entire brain and neck. Neuroradiologists are usually interested in scanning a patient's head from the bottom of the neck to the very top of the head. A possible alternative is to modify the petal coil geometry to form an ellipse or rectangular petal coils to make it possible to fully cover the head for greater volume scans. These geometries can cover the volume in a more efficient and practical fashion.

Both phantom and brain images reveal hyperintensities that are caused by the small petal coils. Small coils can acquire high signals, because small regions produce very little noise. Hyperintensities drastically alter the uniformity image, making it necessary to apply an image-correction algorithm as in the case of images obtained with phased-array coils. These image-correction algorithms should mask the hyperintensities in order to improve the image quality and reveal important anatomical structures of the brain disease. There is a great abundance of image-processing methods to correct bad MR image uniformity in the literature. However, this image processing task is beyond the scope of this paper.

The results presented here show that a resonator volume design can be developed based entirely on the principles of the petal resonator coil for applications in MR neuroimaging. The simple geometries used in this design facilitate the construction and design of other configurations of petal-resonator designs, since the coil performance of common configurations is well understood. Imaging experiments have shown that General Electric MR imagers have great versatility and compatibility with coil prototypes developed by external groups.

5. Conclusion

A volume coil prototype based on the petal resonator surface coil was developed and tested on a clinical MR imager. The petal resonator volume coil can generate brain images with good quality. It is fully compatible with the standard imaging sequences found in most clinical scanners. The principles of the petal resonator coil provide a good alternative to the trial-and-error approach to reliably develop MRI volume

coils. This design approach has a wide range of possible configurations that can generate a higher *SNR* than the popular volume coils. We are convinced that this approach to receive-only coils can be extended to other parts of the human body, as well as be exploited in ultra fast imaging sequences like SENSE, SMASH and phased-array coil imaging.

Acknowledgments

Authors wish to express their gratitude to the American British Cowdray Hospital Tacubaya, General Electric Sistemas Médicos México and Schering Mexicana for their invaluable support for this research. We also thank the Secretariat of Public Education (FOMES-SEP) for a research grant: P/FPMES 98-35-11, DES UAM 98-05. SS would like to thank to CONACYT-Mexico for a Ph D scholarship. Support from Inovamédica is gratefully acknowledged.

-
- * Corresponding author.
 - ** Present Address: Imaging Research Laboratories, Robarts Research Institute, 100 Perth Drive, London, Ontario, CANADA N6A5K8.
1. J. Tropp, *J. Magn. Reson.* **167** (2004) 12.
 2. J.T. Vaughan *et al.*, *Magn. Reson. Med.* **47** (2002) 990.
 3. P. Jursinic, R. Prost, and C.A. Schultz, *J. Neurosurg.* **97** (5 Suppl) (2002) 563.
 4. L.L. Wald, S.E. Moyher, M.R. Day, S.J. Nelson, and D.B. Vigneron, *Magn. Reson. Med.* **34** (1995) 440.
 5. K.M. Welker, J.S. Tsuruda, J.R. Hadley, and C.E. Hayes, *Radiology* **221** (2001) 11.
 6. X. Zhang, K. Ugurbil, and W. Chen, *J. Magn. Reson.* **161** (2003) 242.
 7. J.A. de Zwart, P.J. Ledden, P. Kellman, P. van Gelderen, and J.H. Duyn, *Magn. Reson. Med.* **47** (2002) 1218.
 8. A. Rodriguez, R. Rojas, and F.A. Barrios, *J. Magn. Reson. Imaging.* **13** (2001) 813.
 9. A.O. Rodriguez, S. Hidalgo, R. Rojas, and F.A. Barrios, *Magnetic Resonance Imaging*, **23** (2005) 1027.
 10. A.O. Rodriguez and L. Medina, *Phys. Med. Biol.* **50**(2005) N1.
 11. P. Mansfield, *J Phys D: Appl Phys* **21** (1988) 1643.
 12. J. Wang, A. Reykowski, and J. Dickas, *Trans. Biomed. Eng.* **42** (1995) 908.
 13. S.O. Mitchell, Acceptance Testing: procedure and phantoms, in Dixon, RI, MRI: Acceptance testing and quality control. The role of the medical physicist., *Proc. AAPM Symposium* (Medical Physics Publishing Co., Madison, 1988) pp. 98-114.
 14. R. Hernández, A.O. Rodriguez, P. Salgado, and F.A. Barrios, *Rev. Mex. Fís.* **49** (2003) 107.